Conference Paper

Performance and Limitations of the Conventional Electrode Materials for Erosion of High Aspect Ratio Microcavities

Author(s):
Maradia, Umang; Taborelli, M.; Boos, J.; Buettner, H.; Stirnimann, J.; Boccadoro, M.; Wegener, Konrad

Publication Date:
2016

Permanent Link:
https://doi.org/10.3929/ethz-a-010608880 →

Originally published in:
Procedia CIRP 42, http://doi.org/10.1016/j.procir.2016.02.220 →

Available online at www.sciencedirect.com

ScienceDirect

Procedia CIRP 42 (2016) 606 – 611

www.elsevier.com/locate/procedia

18th CIRP Conference on Electro Physical and Chemical Machining (ISEM XVIII)

Performance and limitations of the conventional electrode materials for erosion of high aspect ratio microcavities

U. Maradia[a,*], M. Taborelli[b], J. Boos[a], H. Buettner[a], J. Stirnimann[a], M. Boccadoro[b], K. Wegener[a,c]

[a]*inspire AG, Leonhardstrasse 21, LEE L205, Zurich 8092, Switzerland*
[b]*GF Machining Solutions, Losone 6616, Switzerland*
[c]*Institute of Machine Tools and Manufacture, ETH Zurich, Zurich 8092, Switzerland*

* Corresponding author. Tel.: +41-446329136 ; fax: +41-446321125. *E-mail address:* maradia@inspire.ethz.ch

Abstract

The low electrode wear strategy based on a carbonaceous layer formation on electrodes considerably increases resource efficiency in the conventional die-sinking EDM. However, the smallest electrode projection area A_p for using the strategy is limited to 0.1 mm^2 and maximum pulse current 3A, possibly due to the pulse re-opening phenomenon. In this work, using a novel generator circuit, pulse re-openings have been restricted up to pulse durations 100 µs and a current of 1A. Hence, the performance of conventional electrode materials is evaluated in order to push the limits of the low wear strategy. However, when using graphite and copper infiltrated graphite microelectrodes, bending of the electrodes is observed, especially in the tip region. The simulation of temperature in the microelectrodes suggests abnormal carbonaceous build up process. This explanation is also concurrent to the observation of a process instability resulting in irreproducible electrode wear behaviour. For copper microelectrodes, another phenomenon is observed where overcuts are produced in the eroded cavities. These overcuts are produced by sparks with high discharge voltage. Sliding of the plasma channel from the electrode corners to the side surfaces is proposed to cause such discharges and overcuts. Thus, underlying mechanisms limiting the low wear strategy in micro-EDM are identified.

Peer-review under responsibility of the organizing committee of 18th CIRP Conference on Electro Physical and Chemical Machining (ISEM XVIII)

Keywords: Micro-EDM; Electrode wear; Micromachining

1. Introduction

Electrode wear is one of the main challenges for resource efficient implementation of die-sinking EDM in micromachining. Hence, several methods have been developed to reduce the electrode wear, such as coating of electrodes in [1], the use of high boiling point - high thermal conductivity materials in [2] and wear compensation in micro-EDM milling in [3]. Nonetheless, the most common industrial approach is similar to that used in the conventional die-sinking EDM, i.e. multiple electrode strategy. In conventional EDM, zero-wear strategies developed in [4] utilising formation of a carbonaceous layer during erosion have reduced graphite and copper electrode wear to near zero values. Such strategies have been further extended to meso-micro scale erosion in [5]. However, currently the method is limited to a minimum dimension of the electrode cross section of 0.3mm × 0.3mm (projection area A_p ~0.1mm^2).

For a low wear strategy, max. current 20A is applied in [5] to Ø0.8 mm graphite electrodes. Assuming a linear correlation between the electrode surface area and maximum current, one sees in Fig. 1 that the maximum current for the electrode diameters below 0.3 mm is below 3A. However, for the positive electrode polarity and transistor type pulses of several microsecond durations, the re-opening phenomenon occurs, which considerably increases the electrode wear as explained below. Thus, pulse re-opening phenomenon may have limited the ability to implement low wear strategy for using the electrodes with side dimensions below 0.3 mm.

Peer-review under responsibility of the organizing committee of 18th CIRP Conference on Electro Physical and Chemical Machining (ISEM XVIII)
doi:10.1016/j.procir.2016.02.220

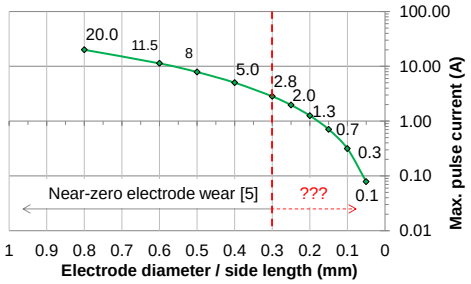

Fig. 1. The maximum applicable current according to the electrode diameter or side length for achieving near-zero electrode wear for graphite and copper.

In this work, the performance of conventional electrode materials, graphite and copper is analysed regarding the implementation of a low wear strategy for smallest A_p 0.01 mm^2, by preventing pulse re-openings. Followed by the explanation of pulse re-opening phenomenon, the experimental setup and methods is presented. The electrode wear behaviour and process stability are presented subsequently.

1.1. Pulse re-opening

For the current pulses generated by a transistor type generator, the use of lower current often results in pulse break before the set pulse duration. This phenomenon is termed as pulse re-opening. An illustration of voltage and current waveform is presented in Fig. 2 (left). Here, the OCP signal is a combination of pulse delay time T_d and set pulse duration T_{ON}. It is seen that during the set pulse duration, the current falls to zero on two separate occasions after the discharge breakdown. At the same time, the voltage value is similar to the ignition voltage. This situation represents an open circuit, i.e. the current conducting plasma channel is absent between the electrode and workpiece. Since each rising edge of the current and resultant short pulse duration causes wear, higher electrode wear is observed when eroding with lower currents due to the re-openings. The current value below which the re-openings occur frequently also depends on the electrode surface area. The frequency and duration after which the pulse re-opening occurs is stochastic. This is evident in Fig. 2 (right), where voltage and current signals of discharges are superimposed for 5 ms when eroding in the pulse re-opening regime (I <3A). When the current amplitude consists of transistor switching noise, the pulse re-opening occurs when the current is lower than the average current amplitude.

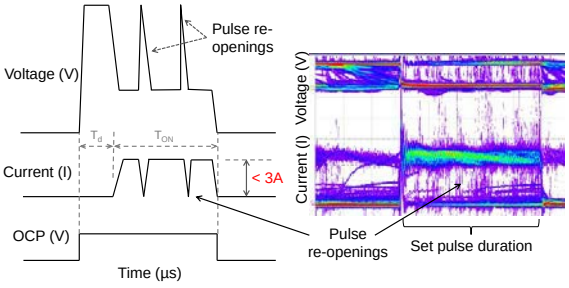

Fig. 2. Left: illustration of voltage and current signals during pulse re-opening. Right: voltage and current signals superimposed for 5 ms.

2. Experimental setup and methods

2.1. Equipment and materials

A die-sinking EDM machine Form 2000 from GF Machining Solutions is used for the erosion experiments. Dielectric oil Oelheld IME110 with a kinematic viscosity of 3.4 mm^2/s (at 20°C) and density 0.78 g/cm^3 (at 15°C) is used. Hot-working steel 1.2343 is used as workpiece material. Graphite (Poco EDM-3, average particle size < 5 µm), copper infiltrated graphite (Poco EDM-C3, average particle size < 5 µm) and pure copper are used as electrode materials. In EDM-C3, copper is filled in the pockets between graphite particles (see Fig. 3), which increases thermal and electrical conductivity of the material, as seen in Table 1. EDM-3 and EDM-C3 electrodes have been milled to the cross-section dimensions of 0.2 mm × 0.2 mm and 0.1 mm × 0.1 mm and length of 5 mm. Since milling of copper microelectrodes with high-aspect ratio was not feasible, copper electrodes with smallest cross-section of 0.3 mm × 0.3 mm and length of 3 mm are prepared using wire-EDM.

2.2. Erosion parameters

High generator impedance may result in a resonant circuit, causing significantly higher ignition voltage, which may lead to the discharge breakdown even in larger gaps, causing pulse re-openings. In order to avoid the pulse re-opening phenomenon for currents below 3A, a modified electrical circuit is used to reduce the isopulse generator impedance. It is seen in Fig. 4 that compared to the standard generator performance, the modified configuration completely averts the pulse re-openings for 2A, whereas reduces the re-opening events considerably for 1.5A and 1A, up to the set pulse duration of 87 µs. An open circuit voltage U_i of 100V with positive electrode polarity is used for all the experiments. Servo control is based on the measured discharge voltage. The pause duration is kept constant at 1000 µs. The flushing cycle, i.e. electrode jump is applied after 100 ms of erosion time.

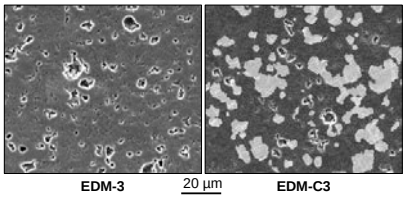

Fig. 3. Microstructure of Poco EDM-3 graphite (left) and copper infiltrated graphite Poco EDM-C3 (right).

Table 1. Comparison of relevant properties of the electrode materials.

Electrode material	EDM-3	EDM-C3	Copper
Density ρ (g/cm^3)	1.81	3.05	8.96
Thermal conductivity k (W/m·K)	95	175	401
Specific heat C_p (J/Kg·K)	710	650*	385
Sublimation/Melting (K)	3650	1358	1358
Electrical resistivity (µΩ·m)	15.6	3.2	0.04

*Assumed value due to unavailability of data

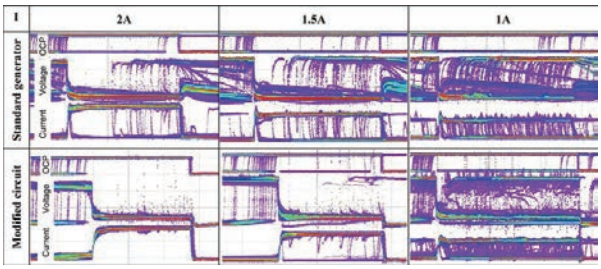

Fig. 4. Comparison of voltage and current waveforms resulting from the standard machine generator and the modified electric circuit configuration with low generator impedance, for currents 2A, 1.5A and 1A. The signals are superimposed in persistence mode for a period of 5 ms. Also, on the top of each image, OCP signal is visible which is set for isopulse duration T_{ON} =87 µs.

2.3. Heat conduction simulations

In order to determine the temperature generated in the microelectrodes by single discharges, heat conduction simulations are performed using COMSOL Multiphysics. Here, a 2D axisymmetric model is used, where the electrode radius is 0.05 mm and electrode length is 5 mm, followed by material bulk in order to represent the electrodes used during the experiments and the electrode holder system. A time independent disc heat source with uniform heat flux profile is used. The chosen heat source radius is 6µm for all the simulations, which is derived using the equation provided by [6]. Here, the discharge voltage is 20V, the current is 1A leading to power 20W and the anode energy fraction is assumed to be 0.5.

3. Electrode wear behaviour

3.1. Graphite electrodes

Graphite electrodes with 0.2 mm × 0.2 mm cross-section are used to erode 3 mm deep cavities in steel 1.2343 using 2A. The use of modified electric circuit ensures almost zero pulse re-openings during the erosion. The electrodes after erosion and the top view of eroded cavities are shown in Fig. 5. It is observed that the electrodes have non-uniform wear along the length for T_{ON} above 30µs, when the frontal wear approaches zero or the carbonaceous layer build up occurs. This is shown by two images of each electrode from different sides. Also, for T_{ON} = 100µs, near-zero frontal and lateral wear are achieved with the eroded cavity oversize of 0.95mm. However, a high amount of build-up at T_{ON} = 87µs followed by a build-up height decrease for T_{ON} = 100 µs is atypical. This is further explored in section 4.1.

Furthermore, electrodes with 0.1 mm × 0.1 mm cross section are used to erode 2 mm deep cavities in steel 1.2343. The electrodes after erosion are shown in Fig. 6. It is seen that when eroding with 1A, the electrodes have either strong frontal build-up or high lateral wear. Also, bending of the electrodes, especially in the tip region is observed. In order to understand this effect, two hypotheses have been proposed, namely creep deformation and abnormal carbonaceous build up process, as further investigated in section 3.4.

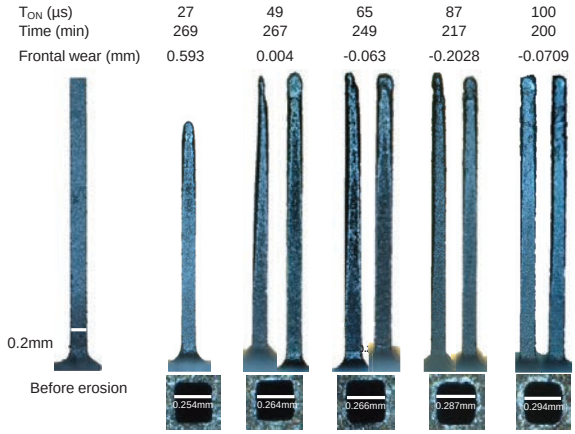

Fig. 5. Graphite electrodes with a cross section of 0.2 mm × 0.2 mm after erosion of 3 mm deep cavities in steel 1.2343 with 2A are shown. Each electrode with two different side views is shown to highlight the non-uniform wear or build-up. Also, top view of the eroded cavities is shown.

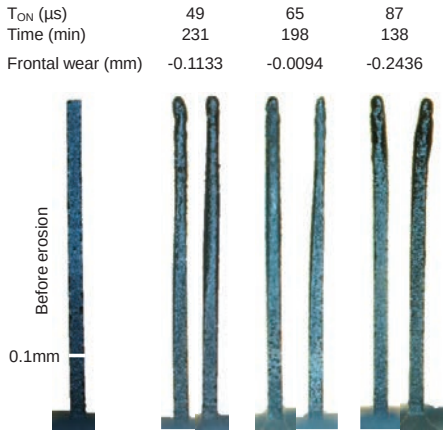

Fig. 6. Graphite electrodes with a cross section of 0.1 mm × 0.1 mm after erosion of 2 mm deep cavities in steel 1.2343 with 1A are shown. Each electrode with two different side views is shown.

3.2. Copper infiltrated graphite electrodes

Electrodes made of EDM-C3 with 0.2 mm × 0.2 mm cross section are used to erode 3 mm deep cavities in steel 1.2343 using 2A. The electrodes after erosion are shown in Fig. 7. It is seen that the electrodes have high lateral wear and also the electrode tip or the built-up tip undergoes bending. Similar effect is also observed on the electrodes with cross section 0.1 mm × 0.1mm after erosion using 1A, as seen in Fig. 8.

3.3. Copper electrodes

A longer pulse duration is required to achieve near-zero wear for copper microelectrodes as shown by [4]. In this work, a square section copper electrode with side length 0.3 mm is used for erosion of 3 mm deep cavity in steel 1.2343 with 3A. Using T_{ON} = 274 µs, near zero frontal and lateral electrode wear are achieved as shown in Fig. 9. It is seen that during the erosion process, a thin black layer is generated over the copper electrode frontal and lateral surfaces.

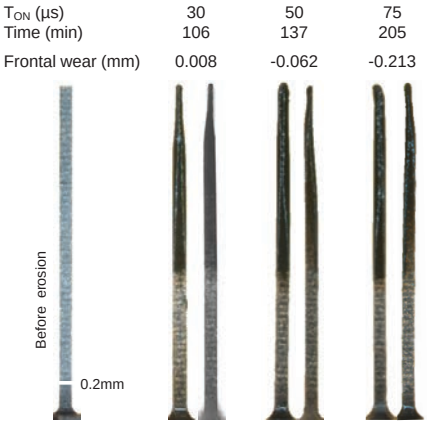

Fig. 7. Copper infiltrated graphite electrodes with a cross section of 0.2 mm × 0.2 mm after erosion of 3 mm deep cavities in steel 1.2343 with 2A.

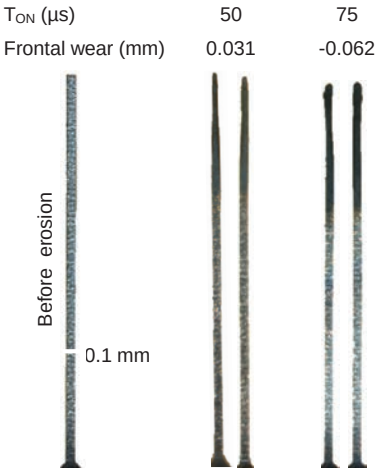

Fig. 8. Copper infiltrated graphite electrodes with a cross section of 0.1 mm × 0.1 mm after erosion of 2 mm deep cavities in steel 1.2343 with 1A.

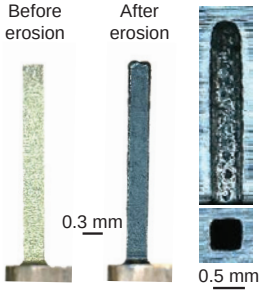

Fig. 9. Copper electrode with 0.3 mm × 0.3 mm cross section after erosion of 3 mm deep cavity in steel 1.2343 using 3 A. The pulse duration is T_{ON} = 274 µs and erosion time is 143 mm. A carbonaceous layer is generated on the electrode surface, with frontal length increase of 7 µm. Cross section and top view of the eroded cavity are also shown.

3.4. Temperature distribution in electrodes

It is observed from the above presented results that both graphite and copper infiltrated graphite microelectrodes, especially with A_p below 0.04 mm^2 undergo irregular carbonaceous build-up and bending of the electrode tip. In order to explain this effect, two hypotheses have been proposed.

It is known that graphite undergoes creep deformation in temperature range 2000°C-3000°C. Here, graphite (EDM-3) and copper infiltrated graphite (EDM-C3) have much lower heat conductivity compared to pure copper. Also, electrical resistivity is relatively high, which might result in higher temperature due to Joule heating. Thus, conduction of heat inside the electrodes might be poor for EDM-3 and EDM-C3 materials, which is analysed using simulations. The simulated temperature along the central axis of Ø0.1 mm electrodes made of the three different materials is presented in Fig. 10. Here, the applied current is 1A, anode energy fraction is considered as 0.5 and the temperatures are shown at T_{ON} = 75µs. It is seen that high temperatures are generated in EDM-3 followed by EDM-C3 and copper. This is obvious since copper has a very high thermal conductivity, thus most of the influx heat is conducted effectively despite of the thin cross section of the electrodes. Also, it has been found that despite the small cross sections, Joule heating for all three materials for the chosen parameters has a negligible effect. Since the region with temperatures above 2000°C is relatively small, heat induced creep deformation is less likely to occur.

Another likely explanation is that the carbonaceous build-up occurs not only on the frontal surface of an electrode but also on the lateral surface at the electrode tip. Such continued lateral build-up results in an inclined build-up volume and may cause process instability. In order to generate carbonaceous build-up over the electrode, [4] have proposed that the electrode surface temperature needs to be higher than the dielectric vaporisation temperature (about 400°C) but below the graphite sublimation temperature. It can be seen Fig. 11 that such temperature regions exist also on the side surfaces of the EDM-3 and EDM-C3 electrodes, facilitating carbonaceous build-up on the side surfaces.

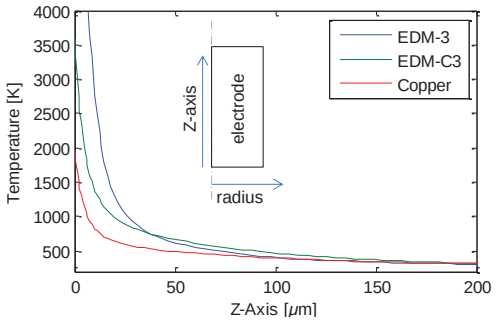

Fig. 10. Temperature along the central axis (Z) of Ø0.1 mm electrodes from the discharge spot for three different electrode materials. Here, discharge voltage is 20V, current 1A, anode energy fraction 0.5 and heat source radius 6 µm. The temperature values shown are at the pulse duration T_{ON} = 75 µs.

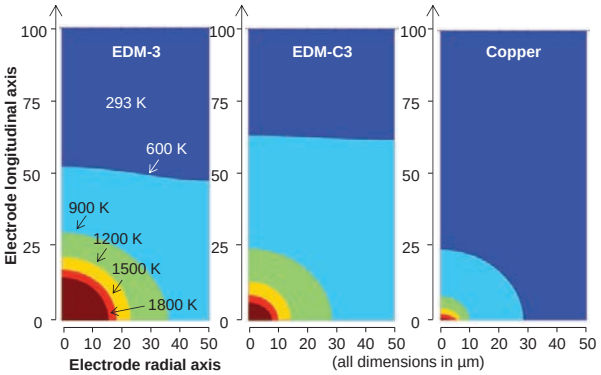

Fig. 11. Isosurface temperature plots of electrodes with 0.5 mm radius and three different materials. The simulation conditions are same as the parameters used above for Fig. 10.

4. Process stability

4.1. Instability

As discussed section 3.1, a 0.2 mm x 0.2 mm cross-section graphite electrode has lower build-up height after the erosion using T_{ON} = 100 µs compared to 87 µs. In order to explain this, electrode axis (Z-axis) movement during the erosion has been analysed as shown in Fig. 12. It is seen that the erosion depth is 3 mm. Here, at two different time instances as highlighted by red ellipses, the Z-axis movement is abrupt and falls suddenly. It can be argued that carbonaceous material is built-up on the electrode frontal surface, and when such build-up has a weak structure, it eventually breaks. Thus, electrode is fed towards the workpiece by the same distance as the height of such built-up peak to adjust the inter-electrode gap. An image of the electrode is shown in Fig. 5 (T_{ON} = 100 µs). Although no such peak is observed on the electrode, Fig. 12 indicates breakage of a peak just before reaching the erosion end at 3 mm erosion depth. Thus, abnormal carbonaceous build-up process is considered to cause the process instability and renders the process non-robust in the low wear parameter domain.

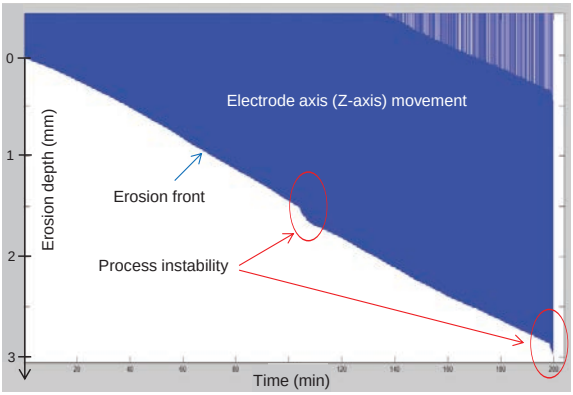

Fig. 12. An example of process instability during the erosion with a 0.2 mm x 0.2 mm graphite electrode, 2A and T_{ON} = 100 µs. An image of the electrode after the erosion is shown in Fig. 5.

4.2. Overcut

Apart from the process instability from the electrode point of view, abnormality has been detected on the workpiece side. Here, overcuts in the machined cavities are observed as shown in Fig. 13(b). Test1 and test2 have been carried out with the same conditions, indicating that the occurrence of an overcut is stochastic. It is also found that the occurrence of such overcuts is much higher when using copper microelectrodes and current below 6A. Also, these overcuts are only visible in the work-piece longitudinal section and not detectable from top view of the eroded cavity.

Although at first, a large pulse duration such as 250 µs is considered to be the main cause, similar defects have been also reported by [7] for the short pulse duration of 15 µs. In order to understand the unstable part of the erosion process, process analysis is carried out where the electrode axis (Z-axis) position and the mean discharge voltage U_e are recorded during the erosion with 32 ms resolution. It is seen in Fig. 14 that along the depth of erosion, when the defect is encountered in the work-piece, the Z-axis retracts away from the workpiece and at the same time, the mean discharge voltage U_e during the erosion rises from about 18 - 20 V to above 36 V.

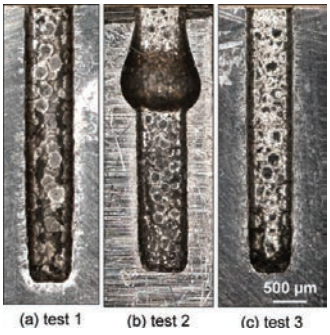

Fig. 13. Longitudinal sections of the cavities eroded using 0.5 mm x 0.5 mm copper electrodes with 5.4 A, T_{ON} = 274 µs. (a) eroded cavity without an overcut; (b) eroded cavity with an overcut caused by the process instability; (c) avoidance of the overcut by the adaptive control proposed by [8].

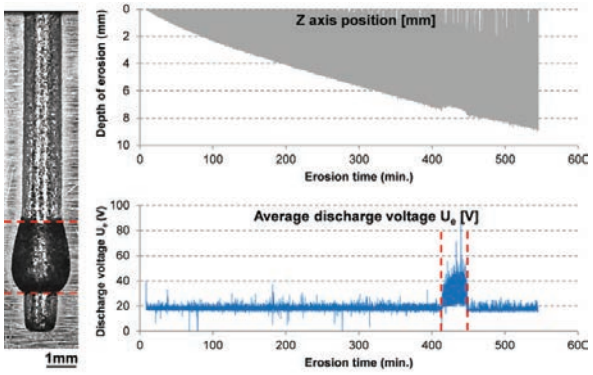

Fig. 14. An example of the process instability causing overcut in the eroded cavity when using a micro scale copper electrode. The electrode axis (Z-axis) position and the mean discharge voltage U_e during the erosion process are correlated, especially the depth at which the overcut is observed.

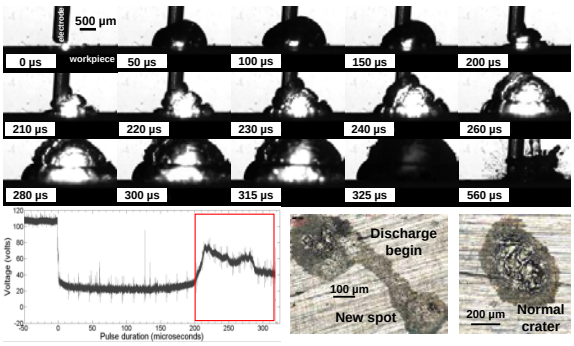

Fig. 15. High-speed photographs of an abnormal discharge generated between a micro copper electrode and steel workpiece. Discharge parameters are 5.4 A current and 316 µs pulse duration.

In order to understand this phenomenon, single discharge experiments using a Ø0.5 mm copper electrode are performed with 5.4 A. High-speed imaging with 200,000 frames per second concurrent to the electrical signal measurements yielded the results shown in Fig. 15. It can be seen from the discharge crater that after the normal discharge phase (till ~200 µs), instability begins within the same discharge, where a spot is created on the cathode at a distance of about 300-500 µm from the begin spot of the discharge breakdown. During the instability phase of the discharge, larger light emission region is seen in addition to more than twice the volume of the gas bubble compared to the normal discharge phase. Also, as opposed to the bubble implosion at the begin spot of the discharge, second collapse takes place at the new spot on the cathode, removing the material at some distance from the original crater. Correlating the crater, voltage signal and visual observations, sparks mostly originating on the electrode corners and having higher discharge voltage are attributed to cause the overcut during erosion. An explanation of this effect is sliding of the discharge spot from the corner to the side of the electrode and also on the work-piece. Since the discharge plasma channel has a certain resistivity, a longer plasma channel will result in the higher discharge voltage. Occurrence of such discharges in series may cause the overcut in the machined cavity. Apart from this, diffuse anode anchoring explained in [9] may also explain both the voltage rise and the crackling sound noted during the occurrence of such discharges. In fact, in order to avoid such instability during the process, adaptive process control as proposed by [8] can be used, where discharges above a certain voltage are terminated upon detection. An example of the eroded cavity using such adaptive control is shown in Fig. 13(c), where similar erosion conditions are used as in the case of tests 1, 2.

5. Conclusions

The performance of graphite, copper infiltrated graphite and copper microelectrodes with projection area A_p as low as 0.01 mm^2 has been analysed in the low wear parameter regime. For the erosion experiments, a modified electric circuit is used to avoid the pulse re-openings which frequently occur for transistor type pulses with currents below 3A, typically required for achieving low wear for A_p < 0.1 mm^2.

For graphite and copper infiltrated graphite microelectrodes:

- For A_p = 0.04 mm^2 and 2A, it is possible to generate carbonaceous build-up layer for T_{ON} > 30 µs. However, the process is not robust, which is explained by an abnormal build up process. Here, relatively thin built-up peaks on the electrode surface might be breaking off during the erosion, making the process unrepeatable.
- For A_p = 0.01 mm^2 and 1A, bending of the electrodes, especially in the tip region is observed. Two hypotheses have been analysed, namely creep deformation and irregular carbonaceous build-up process. Through heat conduction simulations, it is found that the typical temperatures of above 2000°C for graphite creep deformation are limited to a small region. On the other hand, it is seen that carbonaceous layer formation can also occur on the sides of the microelectrodes. Thus, it is likely that lateral build-up on the electrode surfaces causes process instability and electrode bending.

For copper microelectrodes:

- Pulse durations longer than 250 µs are required to achieve near-zero wear. However, overcuts are produced in the eroded cavities when using microelectrodes and current < 6A, which is caused by sparks with U_e >30V. Sliding of the plasma channel on electrode corners may cause this effect.

Acknowledgements

The authors wish to acknowledge the financial support by the Swiss Commission for Technology and Innovation (CTI).

References

[1] Uhlmann E, Roehner M. Investigations on reduction of tool electrode wear in micro-EDM using novel electrode materials. CIRP Journal of Manufacturing Science and Technology. 2008;1(2):92-6.

[2] Tsai Y-Y, Masuzawa T. An index to evaluate the wear resistance of the electrode in micro-EDM. Journal of Materials Processing Technology. 2004;149(1–3):304-9.

[3] Yu Z, Masuzawa T, Fujino M. Micro-EDM for three-dimensional cavities-development of uniform wear method. CIRP Annals-Manufacturing Technology. 1998;47(1):169-72.

[4] Maradia U, Boccadoro M, Stirnimann J, Kuster F, Wegener K. Electrode wear protection mechanism in meso–micro-EDM. Journal of Materials Processing Technology. 2015;223:22-33.

[5] Maradia U, Knaak R, Dal Busco W, Boccadoro M, Wegener K. A strategy for low electrode wear in meso–micro-EDM. Precision Engineering. 2015;42:302-10.

[6] Pandey PC, Jilani ST. Plasma Channel Growth and the Resolidified Layer in Edm. Precis Eng. 1986;8(2):104-10.

[7] Murray J, Zdebski D, Clare AT. Workpiece debris deposition on tool electrodes and secondary discharge phenomena in micro-EDM. Journal of Materials Processing Technology. 2012;212(7):1537-47.

[8] Maradia U, Knaak R, Busco W, Boccadoro M, Stirnimann J, Wegener K. Spark location adaptive process control in meso-micro EDM. Int J Adv Manuf Technol. 2015:1-13.

[9] Raizer Y. Gas discharge physics. Berlin: Springer-Verlag; 1991.